Proceedings of the Korean Nuclear Society Autumn Meeting
Taejon, Korea, October 2000

A Linear Multiple Balance Method for Discrete Ordinates Neutron Transport Equations

Chang Je Park and Nam Zin Cho

Korea Advanced Institute of Science and Technology
Department of Nuclear Engineering
373-1 Kusong-dong, Yusong-gu
Taejon, Korea 305-701

Abstract

A linear multiple balance method (LMB) is developed to provide more accurate and positive solutions for the discrete ordinates neutron transport equations. In this multiple balance approach, one mesh cell is divided into two subcells with quadratic approximation of angular flux distribution. Four multiple balance equations are used to relate center angular flux with average angular flux by Simpson's rule. From the analysis of spatial truncation error, the accuracy of the linear multiple balance scheme is $O(\Delta^4)$ *whereas that of diamond differencing is* $O(\Delta^2)$*. To accelerate the linear multiple balance method, we also describe a simplified additive angular dependent rebalance factor scheme which combines a modified boundary projection acceleration scheme and the angular dependent rebalance factor acceleration scheme. It is demonstrated, via Fourier analysis of a simple model problem as well as numerical calculations, that the additive angular dependent rebalance factor acceleration scheme is unconditionally stable with spectral radius* $< 0.2069c$ *(*c *being the scattering ratio). The numerical results tested so far on slab-geometry discrete ordinates transport problems show that the solution method of linear multiple balance is effective and sufficiently efficient.*

1. Introduction

To provide more accurate and faster solutions for discrete ordinates neutron transport equation, several people have implemented multiple balance schemes or subcell methods. Among multiple balance schemes, Morel and Larsen[1] suggested simple primitive multiple balance methods in early 1990s. They divided a base cell into two subcells and used the standard balance for each discrete spatial cell together with auxiliary equations that represent approximate balance equations over subregions of the cell. Cell edge scalar fluxes are introduced by several ways to approximate balance equations over subregions of the cell. The solutions of primitive multiple balances (PMB, MB-1, and MB-2) are positive and have diffusion limit, but the accuracy is second order as that of diamond differencing. After several years, Castrianni and Adams[2] also suggested new nonlinear multiple balance methods with extension to multi-dimensional geometries. That method, which is algebraically nonlinear, enforces particle conservation on subcells and two multiple balance equations are derived with approximation of the spatial variation of the source in each subcell as an exponential. The half-cell-average fluxes and exiting fluxes are obtained analytically by a transport sweep.

Their solutions are strictly positive and fourth-order accurate, but flawed in thick diffusive and anisotropic problems.

We devise a new linear multiple balance (LMB) method that provides more positive (not strictly positive) and more accurate solutions with reduced extra memory requirement such as cell edge source in the linear characteristic method. Subcell is also considered and four balance equations are used considering two cell edge angular fluxes and two cell center angular fluxes. The source distribution is approximated as spatially linear in a subcell. In addition, the center angular fluxes are introduced as unknowns to approximate the angular fluxes as quadratic distributions. With these additional center angular fluxes, the linear multiple balance scheme developed in this work gives us more accurate solutions than those of the diamond difference (DD) scheme. For simplicity, we consider one-group discrete ordinates neutron transport equation.

In Section 2, we describe the linear multiple balance method for discrete ordinates transport equation. In Section 3, we analyze the spatial truncation errors for the linear multiple balance method and diamond difference method. In Section 4, a diffusion limit analysis is given. To accelerate the linear multiple balance method, an additive angular rebalance factor algorithm is devised in Section 5. In Section 6, we give the numerical results, and in Section 7, we present the conclusions.

2. Derivation of Linear Multiple Balance Method

To describe our linear multiple balance method, we begin with the following one group slab geometry discrete ordinates transport equation in standard notation:

$$\mu_n \frac{d}{dx}\psi_n(x) + \sigma\psi_n(x) = q(x), \tag{1}$$

where

$$\begin{aligned} q(x) &= \sigma_s\phi(x) + S(x), \\ \phi(x) &= \frac{1}{2}\sum_{n=1}^{N} w_n\psi_n(x), \end{aligned} \tag{2}$$

and μ_n and w_n are a discrete ordinate set and its weight, respectively.

Note that $q(x)$ is actually a function of $\psi(x)$, and thus Eq. (1) is solved iteratively with $q(x)$ assumed to be known at each step of the iteration (source iteration). Integrating Eq. (1) over a spatial mesh cell i, of which interval width is $\Delta_i (= x_{i+1/2} - x_{i-1/2})$, we obtain a balance equation as

$$\mu_n(\psi_{i+1/2,n} - \psi_{i-1/2,n}) + \sigma_i\Delta_i\bar{\psi}_{in} = \Delta_i\bar{q}_{in}. \tag{3}$$

Here

$$\begin{aligned} \bar{\psi}_{in} = \frac{1}{\Delta_i}\int_{x_{i-1/2}}^{x_{i+1/2}} \psi(x)dx, \quad \bar{q}_{in} = \frac{1}{\Delta_i}\int_{x_{i-1/2}}^{x_{i+1/2}} q(x)dx, \\ \psi_{i\pm1/2,n} = \psi_n(x_{i\pm1/2}), \quad \sigma_i = \sigma(x_i), \quad x_i = \frac{1}{2}(x_{i-1/2} + x_{i+1/2}). \end{aligned} \tag{4}$$

If $\mu_n > 0$, then particles flow from left to right, and it is appropriate to solve the transport equation following spatial cells in the direction from left to right. Then we can assume that

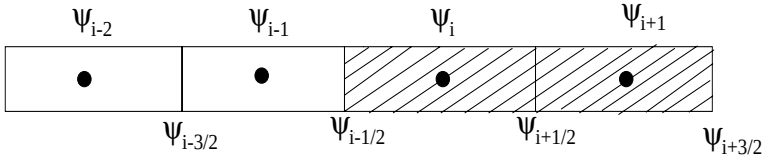

Figure 1: Unknowns of the linear multiple balance method for cell i and $i+1$

$\psi_{i-1/2,n}$ has been determined from the boundary condition or the solution of the previous cell, and that $\bar{q}_{in}$ is known from the previous iteration. Eq. (3) is thus one equation in two unknowns, the cell average flux $\bar{\psi}_{in}$ and the exiting flux $\psi_{i+1/2,n}$.

The diamond difference equation,

$$\bar{\psi}_{in} = \frac{1}{2}(\psi_{i+1/2,n} + \psi_{i-1/2,n}), \tag{5}$$

provides one way to relate $\psi_{i+1/2,n}$ and $\bar{\psi}_{in}$. We may say that the diamond difference (DD) scheme is a linear approximation for angular flux to evaluate cell average flux.

Generally, higher-order approximations for flux may provide more accurate solutions but other flaws can happen such as instability or negativeness of the solutions. A linear multiple balance method is proposed to achieve higher accuracy in additions to more positive and stable properties by assuming a quadratic approximation for angular flux. We apply four balance equations to derive four unknowns; two mesh center angular fluxes and two mesh edge angular fluxes. For example, the balance equations are given at the two subcells (cell i and $i+1$) in Fig. 1.

The four linear multiple balance equations for cell i and $i+1$ are given by

$$\begin{aligned}
&\mu_n(\psi_{i+1/2,n} - \psi_{i-1/2,n}) + \sigma\Delta\frac{\psi_{i-1/2,n} + 4\psi_{i,n} + \psi_{i+1/2,n}}{6} = \Delta\bar{q}_{i,n},\\
&\mu_n(\psi_{i+3/2,n} - \psi_{i+1/2,n}) + \sigma\Delta\frac{\psi_{i+1/2,n} + 4\psi_{i+1,n} + \psi_{i+3/2,n}}{6} = \Delta\bar{q}_{i+1,n},\\
&\mu_n(\psi_{i+3/2,n} - \psi_{i-1/2,n}) + 2\sigma\Delta\frac{\psi_{i-1/2,n} + 4\psi_{i+1/2,n} + \psi_{i+3/2,n}}{6} = \Delta\bar{q}_{i,n} + \Delta\bar{q}_{i+1,n},\\
&\mu_n(\psi_{i+1,n} - \psi_{i,n}) + \sigma\Delta\frac{\psi_{i,n} + 4\psi_{i+1/2,n} + \psi_{i+1,n}}{6} = \frac{\Delta\bar{q}_{i,n} + \Delta\bar{q}_{i+1,n}}{2},
\end{aligned} \tag{6}$$

where $\Delta = \Delta_i = \Delta_{i+1}$, $\sigma = \sigma_i = \sigma_{i+1}$, $\psi_{i,n} = \psi_n(x_i)$. Here, average angular fluxes are expressed by

$$\bar{\psi}_{in} = \frac{1}{\Delta_i}\int_{x_{i-1/2}}^{x_{i+1/2}} \psi_n(x)dx = \frac{\psi_{i-1/2,n} + 4\psi_{i,n} + \psi_{i+1/2,n}}{6}, \tag{7}$$

composed of incoming and outgoing fluxes and center flux using Simpson's rule.

Matrix form for the four balance equations in the linear multiple balance scheme is

$$A\ x = b, \tag{8}$$

where

$$
\begin{aligned}
A &= \begin{pmatrix} 4a & 6+a & 0 & 0 \\ 0 & -6+a & 4a & 6+a \\ 0 & 8a & 0 & 6+2a \\ -6+a & 4a & 6+a & 0 \end{pmatrix}, \\
b &= \begin{pmatrix} 6\frac{\Delta}{|\mu_n|}\bar{q}_{i,n} + (6-a)\psi_{i-1/2,n} \\ 6\frac{\Delta}{|\mu_n|}\bar{q}_{i+1,n} \\ 6\frac{\Delta}{|\mu_n|}(\bar{q}_{i,n} + \bar{q}_{i+1,n}) + (6-2a)\psi_{i-1/2,n} \\ 3\frac{\Delta}{|\mu_n|}(\bar{q}_{i,n} + \bar{q}_{i+1,n}) \end{pmatrix}, \\
x &= \left(\psi_{i,n}, \psi_{i+1/2,n}, \psi_{i+1,n}, \psi_{i+3/2,n}\right)^T, \\
a &= \frac{\sigma\Delta}{|\mu_n|}, \quad |A| = 1728a + 1728a^2 + 720a^3 + 144a^4.
\end{aligned}
\tag{9}
$$

The determinant of the matrix system is positive, and the angular fluxes are obtained by direct inversion.

The effect of the truncation errors or positivity due to the spatial differencing procedure can be seen clearly by examining the case of the uncollided neutrons when the group source is set equal to zero.[3] Eq. (1) reduces to

$$\mu_n \frac{d}{dx}\psi_n(x) + \sigma\psi_n(x) = 0, \tag{10}$$

where we assume a constant cross section. For a uniform grid with mesh spacing Δ, the exact expression for $\psi_{i+1/2,n}$ is

$$\psi_{i+1/2,n} = e^{-2h}\psi_{i-1/2,n}, \tag{11}$$

where

$$h = \frac{\sigma\Delta}{2|\mu_n|}. \tag{12}$$

The diamond difference scheme will give for $\psi_{i+1/2,n}$ as

$$\psi_{i+1/2,n} = \frac{1-h}{1+h}\psi_{i-1/2,n}, \tag{13}$$

whereas the step scheme gives

$$\psi_{i+1/2,n} = \frac{1}{1+2h}\psi_{i-1/2,n}. \tag{14}$$

But the linear multiple balance method gives, by inversion for the matrix system, as

$$
\begin{aligned}
\psi_{i+1/2,n} &= \frac{1}{c_0}\{c1(6-h) + c2(6-2h)\}\psi_{n,i-1/2} \\
&= \frac{12 - 12h + 5h^2 - h^3}{12 + 12h + 5h^2 + h^3}\psi_{n,i-1/2},
\end{aligned}
\tag{15}
$$

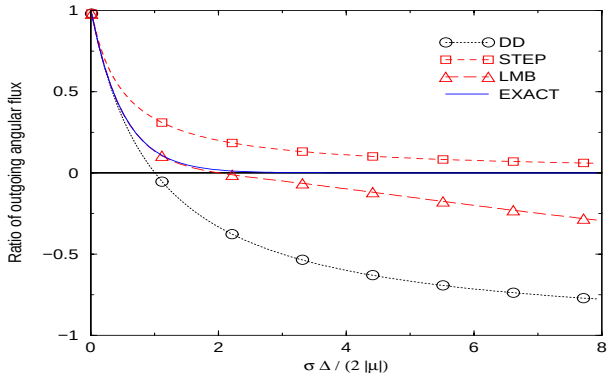

Figure 2: Comparison of the exact solution with three spatial difference approximations

where

$$\begin{aligned} c_0 &= 1728 + 1728h + 720h^2 + 144h^3, \\ c1 &= -192h + 32h^2, \\ c2 &= 288 + 56h^2. \end{aligned} \tag{16}$$

The linear multiple balance method gives more positive solutions than those of the diamond difference scheme as shown in Fig. 2.

3. Convergence Analysis of Linear Multiple Balance Method

In this section, we examine the observed errors, as the spatial mesh size is reduced, for the linear multiple balance method. An analysis of the order of convergence is also provided with Taylor series expansion for slab geometry, one group, discrete ordinates neutron transport equation.

With Taylor series expansion, the numerical integration and differentiation are [4]

$$\begin{aligned} \psi(x_{i+1/2}) &= \psi_i + h\psi_i' + \frac{h^2}{2!}\psi_i'' + \frac{h^3}{3!}\psi_i''' + \cdots, \\ \psi(x_{i-1/2}) &= \psi_i - h\psi_i' + \frac{h^2}{2!}\psi_i'' - \frac{h^3}{3!}\psi_i''' + \cdots, \\ \int_{x_i}^{x_{i-1/2}} \psi(x)dx &= -h\psi_i + \frac{h^2}{2!}\psi_i' - \frac{h^3}{3!}\psi_i'' + \cdots, \\ \int_{x_i}^{x_{i+1/2}} \psi(x)dx &= h\psi_i + \frac{h^2}{2!}\psi_i' + \frac{h^3}{3!}\psi_i'' + \cdots, \\ \int_{x_{i-1/2}}^{x_{i+1/2}} \psi(x)dx &= 2h\psi_i + \frac{h^3}{3}\psi_i'' + \cdots, \\ \psi''(x_i) &= \frac{\psi_{i+1/2} - 2\psi_i + \psi_{i-1/2}}{h^2} - \frac{5h^2}{12}\psi_i^{(iv)} + \cdots, \end{aligned} \tag{17}$$

where $2h = x_{i+1/2} - x_{i-1/2} = \Delta_i$.

Using Eqs. (5) and (17), the spatial truncation error for diamond difference (DD) is derived as

$$\bar{\psi}_i \simeq \frac{1}{2}(\psi_{i+1/2} + \psi_{i-1/2}) - \frac{\Delta_i^2}{24}\frac{d^2\psi}{dx^2}\Big|_{x_i}. \tag{18}$$

Thus, the diamond difference method exhibits $O(\Delta_i^2)$ global cell edge and cell average errors.

To derive the convergence rate for the linear multiple balance method, the twice differential operator terms for angular flux is considered. From Eq. (17), we obtain

$$\psi_{i-1/2} + \psi_{i+1/2} = 2\psi_i + \frac{\Delta_i^2}{4}\psi_i'' + \frac{\Delta_i^4}{232}\psi_i^{iv}, \tag{19}$$

and

$$\bar{\psi}_i \simeq \frac{1}{6}(\psi_{i+1/2} + 4\psi_i + \psi_{i-1/2}) - \frac{\Delta_i^4}{1392}\frac{d^4\psi}{dx^4}\Big|_{x_i}. \tag{20}$$

Thus, the linear multiple balance method exhibits $O(\Delta_i^4)$ global cell edge and cell average errors. To test accuracy of the linear multiple balance method, we select the homogeneous problem described by Larsen and Miller.[5] The one-group and slab geometry problem is solved using the S_2 quadrature set.

$$\begin{aligned} \mu_n \frac{d}{dx}\psi_n(x) + \sigma\psi_n(x) &= \sigma_s \sum_{m=1}^{2} w_m \psi_m(x) + Q, \\ -1 \le x \le 1, &\quad n = 1, 2, \\ \psi_1(-1) = \psi_2(1) &= 0, \end{aligned} \tag{21}$$

where $\sigma = 2,\ \sigma_s = 1,\ \mu_1 = 1/\sqrt{3},\ \mu_2 = -1/\sqrt{3}$, and $w_1 = w_2 = 0.5$.

We also consider a sequence of nine uniform spatial meshes, with $\Delta = 2^{2-n},\ 1 \le n \le 9$. We report the relative errors in the cell edge scalar fluxes:

$$E_{1n} = \max_{0 \le i \le 2^{n-1}} \frac{|\phi_{i+1/2}^{exact} - \phi_{i+1/2}|}{\phi_{i+1/2}^{exact}}, \quad 1 \le n \le 9. \tag{22}$$

Here,

$$\phi_{i+1/2}^{exact} = \frac{1}{2}\left\{\psi_1^{exact}(x_{i+1/2}) + \psi_2^{exact}(x_{i+1/2})\right\}, \quad 0 \le i \le 2^{n-1}, \tag{23}$$

is the exact solution, computed analytically, and $\phi_{i+1/2}$ is the numerical solution. The relative errors of the cell average scalar fluxes are also given by

$$E_{2n} = \max_{0 \le i \le 2^{n-1}} \frac{|\bar{\phi}_i^{exact} - \bar{\phi}_i|}{\bar{\phi}_i^{exact}}, \quad 1 \le n \le 9. \tag{24}$$

Table I shows the cell edge errors(E_{1n}) and cell average errors(E_{2n}) and their error ratios (R_{1n} and R_{2n}). Error ratio is defined by $R_{kn} = E_{k,n-1}/E_{kn}, \quad k = 1, 2$. The results indicate the second-order (DD) and fourth-order (LMB) accuracies by providing the error ratios of 4 and 16, respectively, for sufficiently fine meshes.

Table I: Cell Edge and Cell Average Errors and Error Ratios

	Cell Edge Errors				Cell Average Errors			
	DD		LMB		DD		LMB	
n	E_{1n}	R_{1n}	E_{1n}	R_{1n}	E_{2n}	R_{2n}	E_{2n}	R_{2n}
1	5.4401e-01	—	1.6108e-02	—	1.6903e-01	—	5.0051e-03	—
2	5.4473e-01	0.99	4.8374e-01	0.03	8.5997e-01	0.19	7.8287e-01	0.01
3	4.6557e-02	11.7	1.5942e-02	30.3	3.4035e-02	25.2	6.9789e-03	112
4	1.0927e-02	4.26	1.5831e-03	10.0	1.7639e-02	1.92	1.5113e-03	4.61
5	2.6745e-03	4.08	1.9927e-04	7.94	6.6910e-03	2.63	1.7728e-04	8.52
6	6.6829e-04	4.00	1.8241e-05	10.9	2.1095e-03	3.17	1.5299e-05	11.5
7	1.6678e-04	4.00	1.3996e-06	13.0	5.9693e-04	3.53	1.1270e-06	13.5
8	4.1685e-05	4.00	9.7143e-08	14.4	1.5913e-04	3.75	7.6275e-08	14.7
9	1.0421e-05	4.00	6.1304e-09	15.8	4.1106e-05	3.87	4.6848e-09	16.2

4. Diffusion Limit Analysis of Linear Multiple Balance Method

In strongly diffusing media, the transport equation becomes or has properties of the diffusion equation as an asymptotic limit. Therefore, a diffusion limit analysis for any transport method would provide some assurance that the method has some validity, even if it is not mathematically rigorous as a transport method.

The diffusion the limit analysis for the linear multiple balance scheme is derived similarly to the diamond difference scheme as described in a Larsen's paper.[6]

The balance equation is given as

$$\frac{\mu_n}{h_i}(\psi_{i+1/2,n} - \psi_{i-1/2,n}) + \sigma_i \bar{\psi}_{i,n} = \sigma_{si} \sum_n w_n \bar{\psi}_{i,n} + Q_i. \tag{25}$$

To begin with diffusion limit analysis, the following asymptotic assumptions are needed:

$$\sigma_i \ \rightarrow \ \frac{\sigma_i}{\epsilon}, \quad \sigma_{si} \ \rightarrow \ \frac{\sigma_i}{\epsilon} - \sigma_{ai}\epsilon, \quad Q_i \ \rightarrow \ Q_i\epsilon. \tag{26}$$

Then, the asymptotic balance equation becomes

$$\frac{\mu_n}{h_i}(\psi_{i+1/2,n} - \psi_{i-1/2,n}) + \frac{\sigma_i}{\epsilon}\bar{\psi}_{i,n} = (\frac{\sigma_i}{\epsilon} - \epsilon\sigma_{ai}) \sum_n w_n \bar{\psi}_{i,n} + \epsilon Q_i. \tag{27}$$

Now, the angular flux may be expressed by a summation of series

$$\psi_n = \sum_{k=0} \epsilon^k \psi_n^{(k)} = \psi_n^{(0)} + \epsilon\psi_n^{(1)} + \epsilon^2\psi_n^{(2)} + \cdots . \tag{28}$$

First, collecting terms for $O(1/\epsilon)$,

$$\begin{aligned} &\sigma_i(\bar{\psi}_{i,n}^{(0)} - \sum_n w_n \bar{\psi}_{i,n}^{(0)}) = 0, \\ &\bar{\psi}_{i,n}^{(0)} = \bar{\phi}_i^{(0)}. \end{aligned} \tag{29}$$

Second, collecting terms for $O(1)$,

$$\begin{aligned}\sigma_i(\bar{\psi}^{(1)}_{i,n} - \sum_n w_n \bar{\psi}^{(1)}_{i,n}) &= -\frac{\mu_n}{h_i}(\psi^{(0)}_{i+1/2,n} - \psi^{(0)}_{i-1/2,n}),\\ \bar{\psi}^{(1)}_{i,n} &= \bar{\phi}^{(1)}_i - \frac{\mu_n}{\sigma_i h_i}(\psi^{(0)}_{i+1/2,n} - \psi^{(0)}_{i-1/2,n}).\end{aligned} \tag{30}$$

Finally, for $O(\epsilon)$,

$$\sigma_i(\bar{\psi}^{(2)}_{i,n} - \sum_n w_n \bar{\psi}^{(2)}_{i,n}) = -\frac{\mu_n}{h_i}(\psi^{(1)}_{i+1/2,n} - \psi^{(1)}_{i-1/2,n}) - \sigma_{ai}\sum_n w_n \bar{\psi}^{(0)}_{i,n} + Q_i. \tag{31}$$

If solvability condition is applied by summing Eq. (31) over w_n, then

$$\begin{aligned}\sum_n w_n\mu_n(\psi^{(1)}_{i+1/2,n} - \psi^{(1)}_{i-1/2,n}) &= -\sigma_{ai}h_i\bar{\phi}^{(0)}_i + h_iQ_i,\\ \sum_n w_n\mu_n(\psi^{(1)}_{i+3/2,n} - \psi^{(1)}_{i+1/2,n}) &= -\sigma_{a,i+1}h_{i+1}\bar{\phi}^{(0)}_{i+1} + h_{i+1}Q_{i+1},\\ \sum_n w_n\mu_n(\psi^{(1)}_{i+1,n} - \psi^{(1)}_{i,n}) &= -\sigma_{a,i+1/2}h_{i+1/2}\bar{\phi}^{(0)}_{i+1/2} + h_{i+1/2}Q_{i+1/2}.\end{aligned} \tag{32}$$

Using $\sum_n w_n = 1$, $\sum_n w_n\mu_n = 0$, $\sum_n w_n\mu_n^2 = 1/3$, and $\bar{\psi}_{i,n} = (\psi_{i-1/2,n} + 4\psi_{i,n} + \psi_{i+1/2,n})/6$, we have

$$\begin{aligned}&6\sum_n w_n\mu_n(\bar{\psi}^{(1)}_{i+1,n} - \bar{\psi}^{(1)}_{i,n})\\ &= -\sigma_{a,i}h_i\bar{\phi}^{(0)}_i - 4\sigma_{a,i+1/2}h_{i+1/2}\bar{\phi}^{(0)}_{i+1/2} - \sigma_{a,i+1}h_{i+1}\bar{\phi}^{(0)}_{i+1}\\ &+ h_iQ_i + 4h_{i+1/2}Q_{i+1/2} + h_{i+1}Q_{i+1}.\end{aligned} \tag{33}$$

Combining $O(1)$ and $O(1/\epsilon)$ conditions, we have

$$\begin{aligned}&6\sum_n w_n\mu_n(\bar{\psi}^{(1)}_{i+1,n} - \bar{\psi}^{(1)}_{i,n}) = 6\sum_n w_n\mu_n(\bar{\phi}^{(1)}_{i+1} - \bar{\phi}^{(1)}_i)\\ &- \frac{6}{\sigma_{i+1}h_{i+1}}\sum_n w_n\mu_n^2(\psi^{(0)}_{n,i+3/2} - \psi^{(0)}_{n,i+1/2}) + \frac{6}{\sigma_ih_i}\sum_n w_n\mu_n^2(\psi^{(0)}_{n,i+1/2} - \psi^{(0)}_{n,i-1/2})\\ &= -\frac{2}{\sigma_{i+1}h_{i+1}}(\phi^{(0)}_{i+3/2} - \phi^{(0)}_{i+1/2}) + \frac{2}{\sigma_ih_i}(\phi^{(0)}_{i+1/2} - \phi^{(0)}_{i-1/2}).\end{aligned} \tag{34}$$

From Eqs. (33) and (34), we get

$$\begin{aligned}&-\frac{2}{\sigma_{i+1}h_{i+1}}(\phi^{(0)}_{i+3/2} - \phi^{(0)}_{i+1/2}) + \frac{2}{\sigma_ih_i}(\phi^{(0)}_{i+1/2} - \phi^{(0)}_{i-1/2}) + \sigma_{a,i}h_i\bar{\phi}^{(0)}_i\\ &+ 4\sigma_{a,i+1/2}h_{i+1/2}\bar{\phi}^{(0)}_{i+1/2} + \sigma_{a,i+1}h_{i+1}\bar{\phi}^{(0)}_{i+1} = h_iQ_i + 4h_{i+1/2}Q_{i+1/2} + h_{i+1}Q_{i+1}.\end{aligned} \tag{35}$$

Thus, we have a diffusion-like form for the linear multiple balance method.

5. Acceleration of Linear Multiple Balance Method

Various algorithms have been developed to accelerate the source iteration for discrete ordinates equation. Among these algorithms, the diffusion synthetic acceleration (DSA)[7]

is most popular and unconditionally stable and rapidly convergent. Recently transport synthetic acceleration (TSA)[8], boundary projection acceleration (BPA)[9], and angular dependent rebalance (ADR)[10] factor acceleration methods were developed. These schemes have generality with respect to geometry, discretization scheme, and mesh shape.

To accelerate the linear multiple balance scheme, it is not trivial to derive DSA for center angular flux. So we develop an additive angular dependent rebalance (AADR) factor algorithm which combines boundary projection acceleration (BPA) and angular dependent rebalance (ADR) factor acceleration. It is found that the effect of acceleration depends on the weighting function ($W_n = 1, \quad |\mu_n|, \quad (|\mu_n|+1)/2, \cdots$) in the additive angular dependent rebalance factor scheme. To solve low-order equation effectively, Bi-CGSTAB algorithm is used.

Linear multiple balance equations at $l+1/2$ iteration is given by

$$\begin{aligned}
&\mu_n(\psi^{l+1/2}_{i+1/2,n} - \psi^{l+1/2}_{i-1/2,n}) + \sigma\Delta\frac{\psi^{l+1/2}_{i+1/2,n} + 4\psi^{l+1/2}_{i,n} + \psi^{l+1/2}_{i+1/2,n}}{6} = \Delta(\sigma_s\phi^l_i + S_i),\\
&\mu_n(\psi^{l+1/2}_{i+3/2,n} - \psi^{l+1/2}_{i+1/2,n}) + \sigma\Delta\frac{\psi^{l+1/2}_{i+1/2,n} + 4\psi^{l+1/2}_{i+1,n} + \psi^{l+1/2}_{i+3/2,n}}{6} = \Delta(\sigma_s\phi^l_{i+1} + S_{i+1}),\\
&\mu_n(\psi^{l+1/2}_{i+3/2,n} - \psi^{l+1/2}_{i-1/2,n}) + 2\sigma\Delta\frac{\psi^{l+1/2}_{i-1/2,n} + 4\psi^{l+1/2}_{i+1/2,n} + \psi^{l+1/2}_{i+3/2,n}}{6} = \Delta(\sigma_s\phi^l_i + \sigma_s\phi^l_{i+1} + S_i + S_{i+1}),\\
&\mu_n(\psi^{l+1/2}_{i+1,n} - \psi^{l+1/2}_{i,n}) + \sigma\Delta\frac{\psi^{l+1/2}_{i,n} + 4\psi^{l+1/2}_{i+1/2,n} + \psi^{l+1/2}_{i+1,n}}{6} = \frac{\Delta}{2}(\sigma_s\phi^l_i + \sigma_s\phi^l_{i+1} + S_i + S_{i+1}),
\end{aligned} \tag{36}$$

and

$$\begin{aligned}
\phi^{l+1/2}_i &= \frac{1}{2}\sum_{n=1}^{N} w_n \frac{\psi^{l+1/2}_{i-1/2,n} + 4\psi^{l+1/2}_{i,n} + \psi^{l+1/2}_{i+1/2,n}}{6},\\
\phi^{l+1/2}_{i+1} &= \frac{1}{2}\sum_{n=1}^{N} w_n \frac{\psi^{l+1/2}_{i+1/2,n} + 4\psi^{l+1/2}_{i+1,n} + \psi^{l+1/2}_{i+3/2,n}}{6}.
\end{aligned} \tag{37}$$

Considering rebalance factor in DP_0 form,

$$\begin{aligned}
\psi^{l+1}_{i,n} &= \psi^{l+1/2}_{i,n} + f^{+,l+1}_i, \quad \mu_n > 0,\\
\psi^{l+1}_{i,n} &= \psi^{l+1/2}_{i,n} + f^{-,l+1}_i, \quad \mu_n < 0,
\end{aligned} \tag{38}$$

then multiple balance equations at $l+1$ iteration become

$$\begin{aligned}
&\mu_n(\psi^{l+1}_{i+1/2,n} - \psi^{l+1}_{i-1/2,n}) + \sigma\Delta\frac{\psi^{l+1}_{i+1/2,n} + 4\psi^{l+1}_{i,n} + \psi^{l+1}_{i+1/2,n}}{6} = \Delta(\sigma_s\phi^{l+1}_i + S_i),\\
&\mu_n(\psi^{l+1}_{i+3/2,n} - \psi^{l+1}_{i+1/2,n}) + \sigma\Delta\frac{\psi^{l+1}_{i+1/2,n} + 4\psi^{l+1}_{i+1,n} + \psi^{l+1}_{i+3/2,n}}{6} = \Delta(\sigma_s\phi^{l+1}_{i+1} + S_{i+1}),\\
&\mu_n(\psi^{l+1}_{i+3/2,n} - \psi^{l+1}_{i-1/2,n}) + 2\sigma\Delta\frac{\psi^{l+1}_{i-1/2,n} + 4\psi^{l+1}_{i+1/2,n} + \psi^{l+1}_{i+3/2,n}}{6} = \Delta(\sigma_s\phi^{l+1}_i + \sigma_s\phi^{l+1}_{i+1} + S_i + S_{i+1}),\\
&\mu_n(\psi^{l+1}_{i+1,n} - \psi^{l+1}_{i,n}) + \sigma\Delta\frac{\psi^{l+1}_{i,n} + 4\psi^{l+1}_{i+1/2,n} + \psi^{l+1}_{i+1,n}}{6} = \frac{\Delta}{2}(\sigma_s\phi^{l+1}_i + \sigma_s\phi^{l+1}_{i+1} + S_i + S_{i+1}).
\end{aligned} \tag{39}$$

Subtracting Eq. (36) from Eq. (39) and summing over weighting function W_n, we obtain

the rebalance equations as, for $\mu_n > 0$,

$$\begin{aligned}
&k_1(f_{i+1/2}^{+,l+1} - f_{i-1/2}^{+,l+1}) + k_0\sigma\Delta\frac{f_{i-1/2}^{+,l+1} + 4f_i^{+,l+1} + f_{i+1/2}^{+,l+1}}{6} = k_0\Delta\sigma_s(\phi_i^{l+1} - \phi_i^l),\\
&k_1(f_{i+3/2}^{+,l+1} - f_{i+1/2}^{+,l+1}) + k_0\sigma\Delta\frac{f_{i+1/2}^{+,l+1} + 4f_{i+1}^{+,l+1} + f_{i+3/2}^{+,l+1}}{6} = k_0\Delta\sigma_s(\phi_{i+1}^{l+1} - \phi_{i+1}^l),\\
&k_1(f_{i+3/2}^{+,l+1} - f_{i-1/2}^{+,l+1}) + k_0\sigma\Delta\frac{f_{i-1/2}^{+,l+1} + 4f_{i+1/2}^{+,l+1} + f_{i+3/2}^{+,l+1}}{3} = k_0\Delta\sigma_s\{(\phi_i^{l+1} - \phi_i^l) + (\phi_{i+1}^{l+1} - \phi_{i+1}^l)\},\\
&k_1(f_{i+1}^{+,l+1} - f_i^{+,l+1}) + k_0\sigma\Delta\frac{f_i^{+,l+1} + 4f_{i+1/2}^{+,l+1} + f_{i+1}^{+,l+1}}{6} = \frac{k_0}{2}\Delta\sigma_s\{(\phi_i^{l+1} - \phi_i^l) + (\phi_{i+1}^{l+1} - \phi_{i+1}^l)\},
\end{aligned} \tag{40}$$

and for $\mu_n < 0$,

$$\begin{aligned}
&-k_1(f_{i+1/2}^{-,l+1} - f_{i-1/2}^{-,l+1}) + k_0\sigma\Delta\frac{f_{i-1/2}^{-,l+1} + 4f_i^{-,l+1} + f_{i+1/2}^{-,l+1}}{6} = k_0\Delta\sigma_s(\phi_i^{l+1} - \phi_i^l),\\
&-k_1(f_{i+3/2}^{-,l+1} - f_{i+1/2}^{-,l+1}) + k_0\sigma\Delta\frac{f_{i+1/2}^{-,l+1} + 4f_{i+1}^{-,l+1} + f_{i+3/2}^{-,l+1}}{6} = k_0\Delta\sigma_s(\phi_{i+1}^{l+1} - \phi_{i+1}^l),\\
&-k_1(f_{i+3/2}^{-,l+1} - f_{i-1/2}^{-,l+1}) + k_0\sigma\Delta\frac{f_{i-1/2}^{-,l+1} + 4f_{i+1/2}^{-,l+1} + f_{i+3/2}^{-,l+1}}{3} = k_0\Delta\sigma_s\{(\phi_i^{l+1} - \phi_i^l) + (\phi_{i+1}^{l+1} - \phi_{i+1}^l)\},\\
&-k_1(f_{i+1}^{-,l+1} - f_i^{-,l+1}) + k_0\sigma\Delta\frac{f_i^{-,l+1} + 4f_{i+1/2}^{-,l+1} + f_{i+1}^{-,l+1}}{6} = \frac{k_0}{2}\Delta\sigma_s\{(\phi_i^{l+1} - \phi_i^l) + (\phi_{i+1}^{l+1} - \phi_{i+1}^l)\},
\end{aligned} \tag{41}$$

where

$$k_0 = \sum_{n=1}^{N/2} W_n w_n, \quad k_1 = \sum_{n=1}^{N/2} W_n w_n |\mu_n|. \tag{42}$$

Cell average scalar flux is obtained using rebalance factors as

$$\phi_i^{l+1} = \phi_i^{l+1/2} + \frac{f_{i+1/2}^{+,l+1} + 4f_i^{+,l+1} + f_{i-1/2}^{+,l+1} + f_{i+1/2}^{-,l+1} + 4f_i^{-,l+1} + f_{i-1/2}^{-,l+1}}{12}. \tag{43}$$

To analyze stability of the additive angular dependent rebalance (AADR) factor algorithm, we define Fourier ansatz:

$$\begin{aligned}
\psi_{i+1/2,n}^{l+1} &= \omega^l A_n e^{i\lambda x_{i+1/2}},\\
f_{i+1/2}^{\pm,l+1} &= \omega^l F_\pm e^{i\lambda x_{i+1/2}},\\
\phi_i^l &= \omega^l B e^{i\lambda x_i},\\
\phi_i^{l+1/2} &= \omega^l C e^{i\lambda x_i}.
\end{aligned} \tag{44}$$

From Eq.(37), we get the following simple equation with coefficients of Fourier ansatz:

$$A_n\left\{i2\mu_n sin\theta + \frac{\sigma\Delta}{6}(2cos\theta + 4)\right\} = \sigma_s\Delta B. \tag{45}$$

From Eq.(38), we also obtain

$$\begin{aligned}
C &= \frac{1}{12}\sum_{n=1}^{N/2} w_n A_n(2cos\theta + 4)\\
&= \frac{1}{12}\sum_{n=1}^{N/2} w_n B\frac{(2cos\theta + 4)\sigma_s\Delta}{i2\mu_n sin\theta + \frac{\sigma\Delta}{6}(2cos\theta + 4)}\\
&= P_1 B,
\end{aligned} \tag{46}$$

where

$$P_1 = \frac{1}{12}\sum_{n=1}^{N/2} w_n \frac{(2cos\theta+4)\sigma_s\Delta}{i2\mu_n sin\theta + \frac{\sigma\Delta}{6}(2cos\theta+4)}. \tag{47}$$

From Eqs. (40) and (41), two relations for the rebalance factors are given by

$$\begin{aligned} F_+ &= \left\{ i2k_1\mu_n sin\theta + k_0\frac{\sigma\Delta}{6}(2cos\theta+4)\right\} = k_0\sigma_s\Delta(\omega-1)C, \quad \mu_n > 0, \\ F_- &= \left\{ i2k_1\mu_n sin\theta + k_0\frac{\sigma\Delta}{6}(2cos\theta+4)\right\} = \sigma_s\Delta(\omega-1)C, \quad \mu_n < 0. \end{aligned} \tag{48}$$

Adding and subtracting Eq.(48) above,

$$\begin{aligned} &(F_+ - F_-)(i2k_1\mu_n sin\theta) + (F_+ + F_-)\left\{ k_0\frac{\sigma\Delta}{6}(2cos\theta+4)\right\} = 2k_0\sigma_s\Delta(\omega-1)B, \\ &(F_+ + F_-)(i2k_1\mu_n sin\theta) + (F_+ - F_-)\left\{ k_0\frac{\sigma\Delta}{6}(2cos\theta+4)\right\} = 0. \end{aligned} \tag{49}$$

We may simplify Eq. (49) as

$$\begin{aligned} &(F_+ - F_-)P_2 + (F_+ + F_-)P_3 = 2k_0\sigma_s\Delta(\omega-1)B, \\ &(F_+ + F_-)P_2 + (F_+ - F_-)P_3 = 0, \end{aligned} \tag{50}$$

where

$$\begin{aligned} P_2 &= i2k_1\mu_n sin\theta, \\ P_3 &= k_0\frac{\sigma\Delta}{6}(2cos\theta+4). \end{aligned} \tag{51}$$

From Eq. (50), we get

$$F_+ + F_- = \frac{P_3}{-P_2^2+P_3^2}2k_0\sigma_s\Delta(\omega-1)B. \tag{52}$$

Combining the above equations, we get a formula for frequency ω.

$$\begin{aligned} \omega C &= P_1 C + \frac{1}{12}(F_+ + F_-)(2cos\theta+4) \\ \omega &= P_1 + \frac{1}{12}(2cos\theta+4)2k_0\sigma_s\Delta\frac{P_3}{-P_2^2+P_3^2}(\omega-1) \\ &= P_1 + P_4(\omega-1) \\ \omega &= \frac{P_1-P_4}{1-P_4}, \end{aligned} \tag{53}$$

where

$$P_4 = \frac{1}{12}(2cos\theta+4)2k_0\sigma_s\Delta\frac{P_3}{-P_2^2+P_3^2}. \tag{54}$$

Finally, spectral radius is obtained by taking maximum value of ω.

Table II: Spectral Radius and Number of Iterations

Methods	Δ	0.01	0.1	1	10
DSA	DD	0.16925(13*)	0.20888(13)	0.20238(12)	0.34051(11)
AADR0 (1**)	DD	0.13129(11)	0.23099(16)	0.32209(20)	0.31471(20)
	LMB	0.13131(11)	0.23101(16)	0.32195(20)	0.32368(20)
AADR1 ($\|\mu\|$)	DD	0.26316(16)	0.27540(17)	0.25229(17)	0.24711(17)
	LMB	0.26317(16)	0.27439(17)	0.25186(17)	0.25640(17)
AADR2 ($(\|\mu\|+1)/2$)	DD	0.17872(13)	0.18931(12)	0.16702(12)	0.38685(11)
	LMB	0.17872(13)	0.18924(12)	0.16150(12)	0.15697(11)

* Number of iterations, ** Weight function

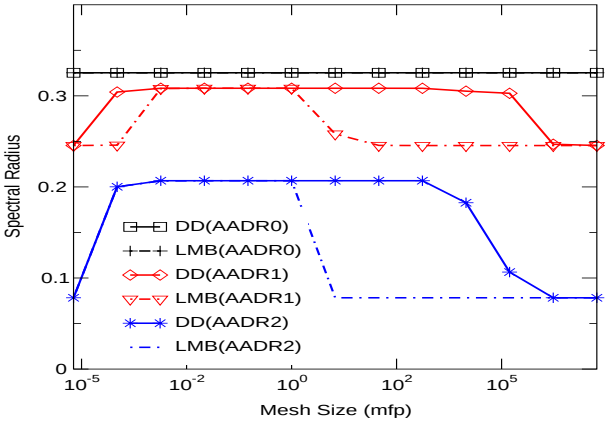

Figure 3: Spectral radius for various mesh cell sizes (mfp)

To assess performance of the additive angular dependent rebalance (AADR) factor acceleration we tested it on a sample problem. Table II shows the numerical spectral radius and number of iterations for a homogeneous slab geometry problem which has $\sigma = \sigma_s = 1$ with vacuum boundary conditions on both sides. The criterion for average scalar flux is given 10^{-9} and S_{16} quadrature is used. The results of AADR2 indicate that it is competitive with or outperform DSA, which results from the use of a proper weighting function. Fig. 3 shows the spectral radius for AADR in the case of linear multiple balance method (LMB) and diamond difference method (DD) from Fourier analysis. As shown in Fig. 3, ADDR with the weighting function $W_n = (|\mu_n| + 1)/2$ gives spectral radius $< 0.2069c$, whereas Larsen's DSA scheme gives spectral radius $< 0.2247c$. The inversion of the low-order equation in AADR is performed by Bi-CGSTAB algorithm, which reduces computational burden.

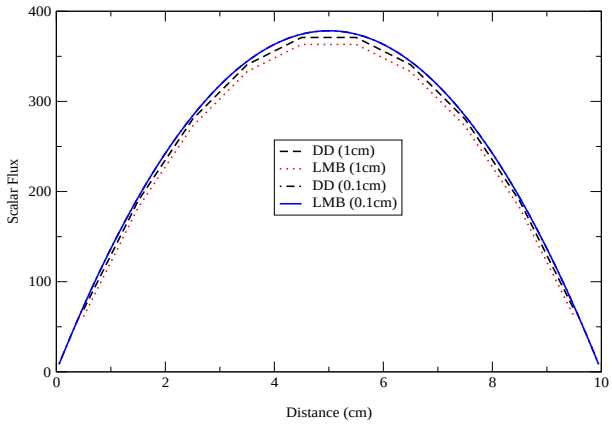

Figure 4: Distribution of scalar flux for optically thick problem

6. Numerical Tests and Results

The first test is an optically thick problem in diffusive regime:[6]

$$\begin{aligned} \mu_n \frac{d}{dx}\psi_n(x) + \sigma\psi_n(x) &= \sigma_s \sum_{m=1}^{8} w_m \psi_m(x) + Q, \\ \sigma = \sigma_s = 100, \quad Q = 0.1, \quad & 0 \le x \le 10cm \\ \psi_n(0) = 0, \quad \mu_n > 0, & \\ \psi_n(10) = 0, \quad \mu_n < 0, \quad & \Delta x = 1cm,\ 0.1cm \end{aligned} \tag{55}$$

The standard S_{16} Gauss-Legendre quadrature set is used. Fig. 4 shows the cell average scalar fluxes for the thick mesh cell and we find that the linear multiple balance method (LMB) has thick diffusion limit as analytically shown.

The second problem we consider is taken from Reed[11] and consists of a slab with four regions with distinct compositions. There is a source of magnitude 50 (arbitrary units) located in the region where the material 1 is placed and a source of magnitude 1 in the region defined by $5 < x < 6$. The slab has reflective boundary condition at the left end and vacuum boundary condition at the right end. The configuration is shown in Fig. 5. This problem is solved with S_8 approximation and error criterion is 10^{-9}. Reference solution is obtained by diamond difference of which mesh size (Δ) is $0.01cm$. The results of diamond difference method, linear multiple balance method, and linear characteristics method are shown in Fig. 6. The diamond difference shows strong oscillations in the optically thickest region because mesh size is too large. For linear multiple balance method as well as linear characteristics method, we can observe that there are little oscillations, due to multiple balances over a spatial cell.

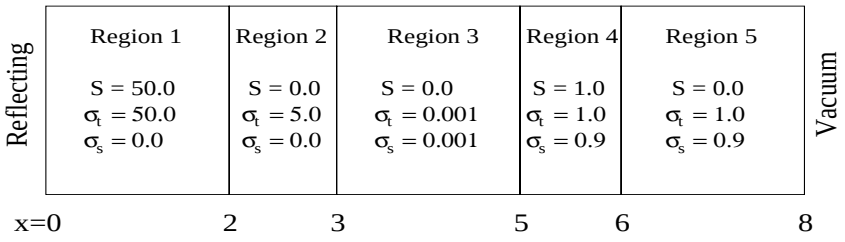

Figure 5: Configuration of Reed problem

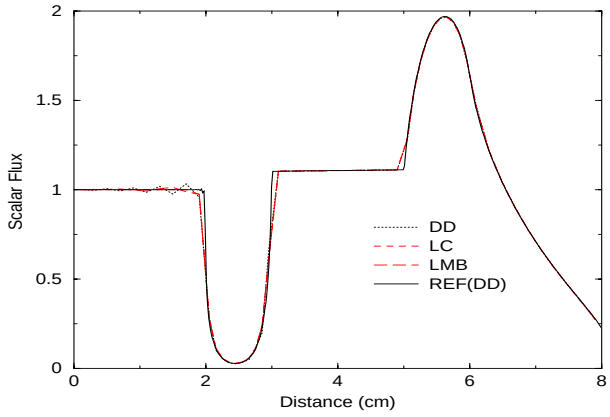

Figure 6: Distribution of scalar flux for Reed problem (mesh size = $0.2cm$)

7. Conclusions

We have developed a new linear multiple balance method (LMB) to get accurate solutions for slab geometry discrete ordinates neutron transport equations. One mesh cell is divided into two subcells with quadratic approximation of angular flux distribution and four multiple balance equations are used to relate center angular flux with average angular flux by Simpson's rule, leading to improved accuracy and positivity. From the error analysis, the orders of cell truncation errors and global cell flux errors are $O(\Delta^4)$ and the numerical results confirmed the accuracy of the method. The method has also diffusion limit and it was accelerated by an additive angular dependent rebalance factor algorithm. Fourier analysis of a simple model problem as well as numerical calculations shows that the additive angular dependent rebalance factor acceleration algorithm is unconditionally stable with spectral radius $< 0.2069c$ when proper weighting functions are used. As a concluding remark, the new linear multiple balance method with additive angular dependent rebalance factor acceleration provides high accuracy and may offer various advantages over the existing methods.

Acknowledgement

This work was supported in part by the Ministry of Science and Technology of Korea through the National Research Laboratory (NRL) Program.

References

[1] J.E. Morel and E.W. Larsen, "A Multiple Balance Approach for Differencing the S_n Equations," *Nucl. Sci. Eng.*, **105**, 1 (1990).

[2] C.L. Castrianni and M.L. Adams, "A Nonlinear Corner-Balance Spatial Discretization for Transport on Arbitrary Grids," *Nucl. Sci. Eng.*, **128**, 278 (1998).

[3] E.W. Larsen and W.F. Miller,Jr., *Computational Methods of Neutron Transport*, John Wiley & Sons (1984).

[4] S.C. Chapra and R.P. Canale, *Numerical Methods for Engineers*, McGraw-Hill (1990).

[5] E.W. Larsen and W.F. Miller,Jr., "Convergence Rates of Spatial Difference Equations for the Discrete-Ordinates Neutron Transport Equations in Slab Geometry," *Nucl. Sci. Eng.*, **73**, 76 (1980).

[6] E.W. Larsen, J.E. Morel, and W.F. Miller,Jr., "Asymptotic Solutions of Numerical Transport Problems in Optically Thick, Diffusive Regimes," *J. Comput. Phys.*, **69**, 283 (1987).

[7] E.W. Larsen, "Unconditionally Stable Diffusion Synthetic Acceleration Method for the Slab Geometry Discrete Ordinates Equations. PartI : Theory," *Nucl. Sci. Eng.*, **82**, 47 (1982).

[8] G.L. Ramone and M.L. Adams, "A Transport Synthetic Acceleration Method for Transport Iterations," *Nucl. Sci. Eng.*, **125**, 257 (1997).

[9] M.L. Adams and W.R. Martin, "Boundary Projection Acceleration : A New Approach to Synthetic Acceleration of Transport Calculations," *Nucl. Sci. Eng.*, **100**, 177 (1988).

[10] S.G. Hong and N.Z. Cho, "Angle-Dependent Rebalance Factor Method for Nodal Transport Problems in X-Y Geometry," *Trans. Am. Nucl. Soc.*, **79**, 139 (1998).

[11] W.H. Reed, "The Effectiveness of Acceleration Techniques for Iterative Methods in Transport Theory," *Nucl. Sci. Eng.*, **46**, 309 (1971).